Experimental test of the Warren-Langer model in nematic-isotropic planar interfaces

O. A. Gomes, N. B. Viana, J. M. A. Figueiredo, and O. N. Mesquita
Departamento de Física, ICEX, Universidade Federal de Minas Gerais, Caixa Postal 702, Belo Horizonte, CEP 30123-970, MG, Brazil
(Received 17 November 1998)

In a directional solidification apparatus, the recoil of the nonsteady planar nematic-isotropic interface of the liquid crystal 8CB doped with hexachloroethane was measured, for different pulling velocities. Results agree very well with the predictions of our two-sided extension of Warren and Langer's one-sided model [Phys. Rev. E **47**, 2702 (1993)], therefore supporting the validity of their ansatz about the evolution of the dopant concentration field. From the comparison between experiment and theory we obtain values for the segregation and diffusion coefficients of hexachloroethane in 8CB comparable to those found in the literature and measured by other methods. Using the same procedure, we measured the value of the segregation coefficient of 8CB doped with water as a function of applied sinusoidal electric field perpendicular to the sample, along the homeotropic direction. The segregation coefficient increases with electric field. In addition, preliminary results on the cellular instability in this system show that the capillary length of the pattern also increases with electric field. To our knowledge, this is the first binary system with continuously tunable segregation coefficient and capillary length. [S1063-651X(99)01905-4]

PACS number(s): 61.30.Gd, 81.30.Fb, 05.70.Ln

I. INTRODUCTION

During directional solidification of alloys morphological instabilities can occur. The initial planar crystal-melt interface can become cellular and dendritic. The linear analysis of this instability was first performed by Mullins and Sekerka [1]. Even though this first analysis was performed 35 years ago and a considerable amount of work, both experimental and theoretical, has been done in this field since then, there are still unanswered questions. Most of the theoretical analysis carried out, including the one by Mullins and Sekerka, assumed that the dopant-concentration field in the alloy attains its dynamic steady-state first, and that only then does the cellular instability set in. Neither linear nor weakly nonlinear perturbation analyses of such a steady state are able to accurately predict the experimentally measured final wavelength of the resulting pattern [2].

Following the original work of Hunt and Jackson [3], experiments on directional solidification are in general performed with quasi-two-dimensional samples between glass slides, in contact with two ovens: one at a temperature above and the other at a temperature below the melting temperature. These temperatures define the temperature gradient, which is a control parameter of the experiment, and are chosen to place the equilibrium crystal-melt interface in the middle of the cell. The crystal-melt interface is observed under a microscope connected to a video-recording system. Suppose that initially the crystal is at rest, and that at time $t=0$ one starts to pull the sample towards the cold oven, with a pulling velocity V_p. The crystal forms, and impurities segregate at the crystal-melt interface. The concentration field is coupled to the temperature field, since the melting temperature varies with impurity concentration at the interface: the more impurities are segregated, the lower the melting temperature. There is a recoil of the interface in the laboratory frame of reference, as the interface accelerates from zero velocity up to the steady-state pulling velocity V_p. Since the time to achieve the steady state can be very long, because of the coupling between thermal and concentration fields, the cellular instability can occur well before the concentration field and interface reach the steady state. Warren and Langer [2] performed a stability analysis of this nonsteady interface. To do that they had to determine the evolution of the concentration field and the interface position. This version of the Stefan problem does not have an analytical solution. They proposed an ansatz to obtain an approximate analytical solution for the evolution of the concentration field and recoil of the interface. The validity of their ansatz was checked by Caroli *et al.* [4] who numerically solved the diffusion equations with a moving boundary appropriate to this problem. Caroli *et al.* concluded that the Warren-Langer ansatz, to be described below, is accurate enough for most experimentally attainable situations. With their nonsteady perturbation analysis and without further mode selection assumptions, Warren and Langer were able to predict the wavelength of the resulting dendritic pattern in the experiments of Trivedi and Somboonsuk [5].

A direct experimental test of the predictions of the Warren-Langer model was recently performed by Losert, Shi, and Cummins [6], for directional solidification of succinonitrile doped with the laser dye Coumarin 152. They found good agreement between their experimental data and the predictions of the Warren-Langer analysis for the evolution of the impurity concentration field, and for the linear growth coefficient of the cellular instability. It was more difficult to test if the recoil of a planar interface as a function of time followed the Warren-Langer model consistently, because the interface, for binary mixtures with low segregation coefficients, takes a very long time to achieve the steady state. In addition, solute trapping at the walls was a problem.

It has been shown that cellular instabilities of nematic-isotropic interfaces of liquid crystals are very similar to instabilities in standard crystal-melt interfaces during directional solidification [7–10]. Experiments with nematic-isotropic interfaces allow the investigation of a range of parameters hardly accessible in standard crystal-melt inter-

faces. In addition, the time scales associated with motion and instabilities of nematic-isotropic interfaces are smaller than those for crystal-melt interfaces, such that during an experimental run we can have a complete evolution of interface positions and instabilities.

The main aim of this article is to check the predictions of the Warren-Langer analysis for the evolution of planar interfaces. Since the original Warren-Langer analysis was proposed for the one-sided model of solidification, where diffusion of impurities in the solid is neglected, in Sec. II we formulate a two-sided version, which is appropriate for nematic-isotropic interfaces, since in this case impurity diffusion can occur in both phases. In Sec. III we describe our experimental method and in Sec. IV we compare the theory with our experimental results.

In addition, we use the method developed in this paper to measure the change in the segregation coefficient when electric field is applied to our liquid crystal sample. The use of electric field to continuously change parameters of liquid crystal binary mixtures can open new possibilities to the study of morphological instabilities in this system.

II. TWO-SIDED EXTENSION OF WARREN-LANGER MODEL

The original Warren-Langer analysis was proposed for the one-sided model of solidification, where diffusion of impurities in the solid is neglected. This is a good approximation for solid-liquid interfaces. Below we extend it to the two-sided model of solidification, which is appropriate for nematic-isotropic interfaces, since in this case impurity diffusion can occur in both phases. We shall only treat the evolution of a flat interface and concomitant buildup of impurities ahead of it.

We start by defining our notation and specifying the various approximations to be used in our analysis. We assume that a two-dimensional description is sufficient. Every point is assumed to be in local thermodynamic equilibrium and kinetic processes at the interface are neglected. We assume that hydrodynamic motion can be neglected [8] so that all transport of solute is diffusive. We further assume that the temperature field is imposed by the experimenter, and that the release of latent heat may be ignored, which is a very good assumption for the weakly first-order nematic-isotropic phase transition. Then the temperature throughout the system is determined by the applied temperature gradient G. We define our coordinate system so that

$$T = T_{NI} + Gz, \tag{1}$$

where z represents the displacement parallel to the direction of motion in a frame moving at the pulling speed V_p with respect to the solidifying material. The temperature T_{NI} is the transition temperature of the pure material.

With these assumptions, the impurity-concentration field obeys a diffusion equation in each phase:

$$D_{N,I}\frac{\partial^2 C_{N,I}}{\partial z^2} + V_p\frac{\partial C_{N,I}}{\partial z} = \frac{\partial C_{N,I}}{\partial t}, \tag{2}$$

where $C_{N,I}(z,t)$ is the time-dependent concentration field of each phase. There are several conditions which must be satisfied at the interface: local phase equilibrium

$$C_N(z_0,t) = kC_I(z_0,t), \tag{3}$$

interface temperature shift by impurity

$$T(z_0) = T_{NI} - mC_I(z_0,t), \tag{4}$$

and mass conservation

$$-D_I\frac{\partial C_I}{\partial z}\bigg|_{z_0} + D_N\frac{\partial C_N}{\partial z}\bigg|_{z_0} = V_0(1-k)C_I(z_0,t), \tag{5}$$

where z_0 is the interface position in the laboratory frame, k is the segregation coefficient, m is the liquidus slope, and V_0 is the velocity of the interface in the frame of reference that is fixed in the solidifying material, that is,

$$V_0(t) = V_p + \dot{z_0}(t). \tag{6}$$

In principle, we must solve the system of Eqs. (2)–(6) for fixed $V_p > 0$ and initial conditions appropriate to the stationary interface at $V_p = 0$. That is,

$$C_I(z,0) = C_\infty, \quad z \geqslant z_0(0),$$

$$C_N(z,0) = kC_\infty, \quad z < z_0(0). \tag{7}$$

We know of no exact analytic solution of this version of the Stefan problem. Note that in the steady state the concentration profile of the flat interface moving at the pulling speed is

$$C_{Ip}(z) = C_\infty + \left[\frac{C_\infty}{k} - C_\infty\right]e^{-2(z-z_\infty/k)/l_{Ip}}, \quad z \geqslant z_\infty/k,$$

$$C_{Np}(z) = C_\infty, \quad z < z_\infty/k, \tag{8}$$

where z_∞ is the position of the interface at $t = 0$

$$z_\infty = -\frac{mC_\infty}{G} \tag{9}$$

and the diffusion length l_{Ip} is

$$l_{Ip} = \frac{2D_I}{V_p}. \tag{10}$$

Following Warren and Langer, with Eq. (8) in mind, we propose an ansatz for the non-steady-state concentration profile, that is,

$$C_I(z,t) = C_\infty + [C_I(z_0,t) - C_\infty]e^{-2(z-z_0)/l_I}, \quad z \geqslant z_0(t),$$

$$C_N(z,t) = k\{C_\infty + [C_I(z_0,t) - C_\infty]e^{2(z-z_0)/l_N}\}, \quad z < z_0(t), \tag{11}$$

where l_I and l_N are isotropic and nematic time-dependent diffusion lengths, respectively. Using the ansatz (11) and Eqs. (2)–(7) we derive equations of motion for z_0, l_I, and l_N:

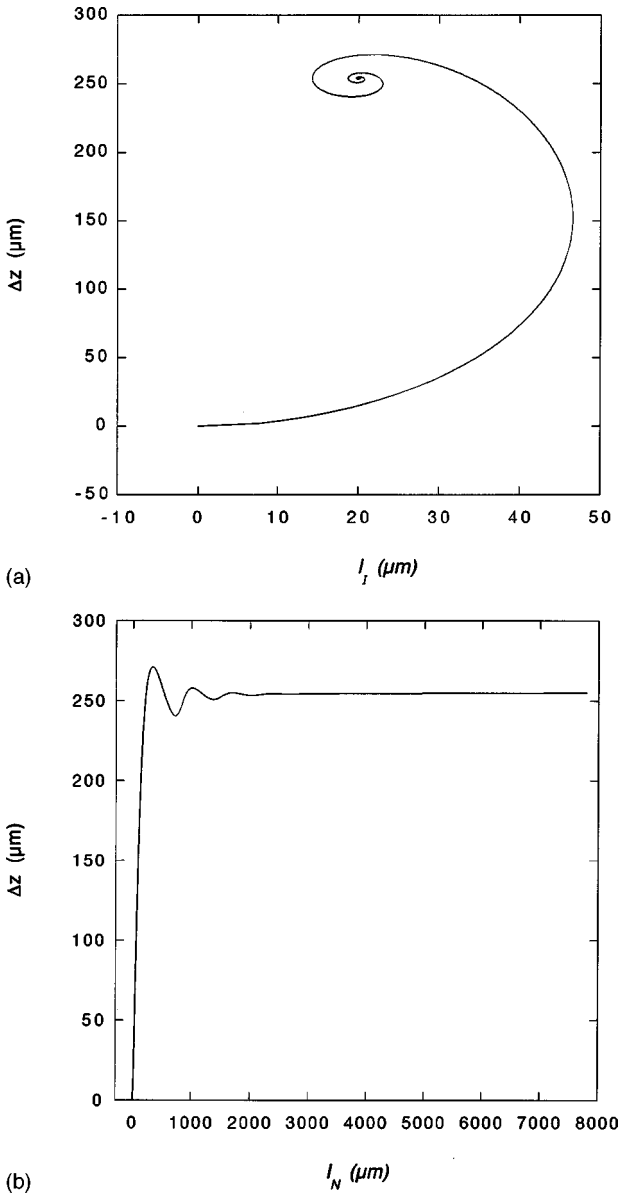

FIG. 1. Trajectory in (a) the $(\Delta z, l_I)$ plane and (b) in the $(\Delta z, l_N)$ plane, for the double-sided model for $V_p = 4.0$ μm/s and $G = 3.0$ K/cm. Δz is the interface position, l_I and l_N are the diffusion lengths in each phase. Parameters are $D_I = 40$ $\mu m^2/s$, $D_N = 20$ $\mu m^2/s$, $C_\infty = 1\%$ molar, and $k = 0.93$.

$$\dot{z}_0 = \left(\frac{2D_I}{l_I} + \frac{2D_N k}{l_N}\right)\frac{z_0 - z_\infty}{(1-k)z_0} - V_p,$$

$$\dot{l}_I = \frac{4D_I(z_\infty - kz_0)}{l_I(1-k)z_0} - \frac{4D_N k(z_0 - z_\infty)}{l_N(1-k)z_0} - \frac{l_I}{z_0 - z_\infty}\dot{z}_0, \quad (12)$$

$$\dot{l}_N = \frac{4D_I(z_0 - z_\infty)}{l_I(1-k)z_0} + \frac{4D_N(z_0 - kz_\infty)}{l_N(1-k)z_0} - \frac{l_N}{z_0 - z_\infty}\dot{z}_0.$$

A numerical solution is shown in Fig. 1(a) and 1(b) in the form of trajectories in the Δz, l_i and Δz, l_n planes, where

$$\Delta z(t) = z_\infty - z_0(t) \quad (13)$$

is the quantity measured in our experiments. To start the numeric computation we use a small t solution for these equations of motion given by

$$l_I = \left(\frac{8D_I t}{3}\right)^{1/2},$$

$$l_N = \left(\frac{8D_N t}{3}\right)^{12}, \quad (14)$$

$$z_0 = z_\infty - V_p t + \frac{V_p\sqrt{2}(\sqrt{D_I} + \sqrt{D_N})}{\sqrt{3}|z_\infty|(1-k)}t^{3/2}.$$

With this procedure we avoid numerical problems at $t = 0$.

Our ansatz consistently sastifies the initial conditions and leads the system to the correct steady-state, given by Eq. (8), since from the dynamics we obtain $l_I(t=\infty) = l_{Ip}$, $l_N(t=\infty) = \infty$ and $z_0(t=\infty) = z_\infty/k$. As shown in Figs. 1(a) and 1(b) $\Delta z(t)$, $l_I(t)$, and $l_N(t)$ present an oscillatory behavior. Such a behavior has not been observed experimentally, presumably because before it happens, the interface has undergone a cellular instability.

At $t \to \infty$ the interface achieves the steady-state and its position remains constant:

$$\Delta z_S = z_\infty - \frac{z_\infty}{k} = \frac{mC_\infty(1-k)}{kG}. \quad (15)$$

The steady-state position Δz_S is independent of pulling velocity. It depends only on concentration of impurity C_∞, the segregation coefficient k, and the temperature gradient G. Later, we will use this result to check our experimental method.

For a comparison of the main differences between our two-sided version and the one-sided Warren-Langer model, in Fig. 2 we show a plot of Δz as a function of time using both the two-sided and one-sided versions: (a) is the result of the two-sided version with parameters $D_I = 40$ $\mu m^2/s$, $D_N = 20$ $\mu m^2/s$, $C_\infty = 1\%$ molar, and $k = 0.93$; (b) is the result of the one-sided version for parameters $D = 40$ $\mu m^2/s$, $C_\infty = 1\%$ molar and $k = 0.93$; (c) is an attempt to fit the two-sided results using the one-sided model. This fit can be made for a limited time interval and gives as a result the parameters $D = 85$ $\mu m^2/s$, $C_\infty = 1\%$ molar, and $k = 0.93$. In this limited time interval the main difference between the one-sided and the two-sided versions is the value for the impurity diffusion coefficient. We will see that in our experiments on the nematic-isotropic interface, attempts to fit the data with the one-sided version gives unacceptably high values for the impurity diffusion coefficient.

III. EXPERIMENTAL METHOD

Most experimental studies on directional solidification of thin samples are based on the original microscopy experiment by Hunt and Jackson [3]. Recent improvements are due to the use of digital-videoimaging techniques. By using an optical microscope with a CCD camera connected to a computer equipped with a frame grabber, we can observe and record the evolution of nematic-isotropic interfaces.

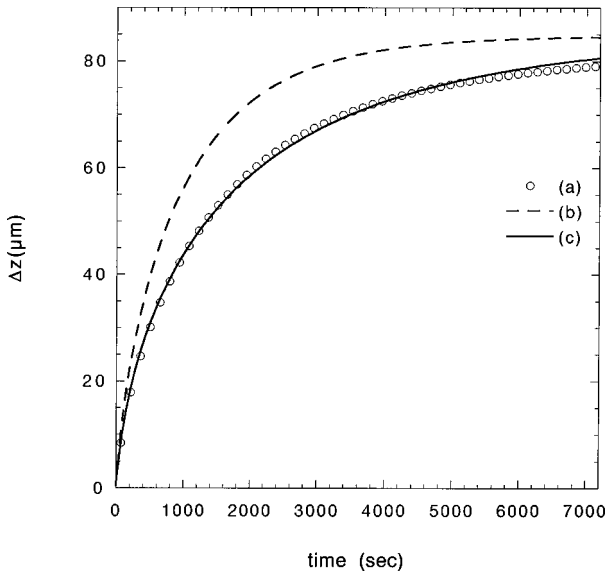

FIG. 2. Interface position as a function of time, showing a comparison between double and one-sided models; (a) is the double-sided model with $D_I=40\ \mu m^2/s$, $D_N=20\ \mu m^2/s$, $C_\infty=1\%$ molar, and $k=0.93$; (b) is the result for the one-sided model using the same parameters ($D=D_I$); (c) is the one-sided fitting to the double-sided values, resulting the parameters $D=85\ \mu m^2/s$, $C_\infty=1\%$ molar, and $k=0.93$.

A. Sample preparation

Our samples are prepared with the liquid crystal 8CB (4-*n*-octylcyanobiphenyl), sandwiched between glass slides with mylar spacers of typically 3.5 μm. The faces of the glass slides in contact with the liquid crystal are covered with a thin film of silane to guarantee a homeotropic configuration for the nematic phase. In the homeotropic configuration the director of the nematic phase is normal to the surfaces of the glass slides [8].

Samples are prepared in a anaerobic chamber, first evacuated and then pressurized with pure argon. We prepared simultaneously a sample with pure 8CB and another with 8CB doped with 1.1% molar of hexachloroethane C_2Cl_6. The pure sample is important to assess the initial concentration of impurities. For a temperature gradient of 9 K/cm the pure sample did not undergo a cellular instability even at our maximum pulling speed of 100 μm/s, while the doped one became unstable for a pulling speed around 3.5 μm/s. Therefore, one can be sure that C_2Cl_6 is the major impurity in our binary system and that other impurities have no effect on the evolution of the interface.

We also use glass slides covered with transparent electrodes of tin oxide produced by CTI [11] in order to apply an electric field to the sample. These slides are silane coated to induce homeotropic orientation.

B. Temperature stability

Our oven consists of a pair of aluminum blocks (7 cm $\times$4 cm$\times$4 cm) separated by a piece of BK7 glass (1.1 cm $\times$ 4 cm $\times$ 4 cm). The sample is pressed against the blocks in a controlled way with a cover glass with foam pieces. This assures good thermal contact and a smooth sliding of the sample. The whole system is tightly enclosed in an insulating box with glass windows for illumination and observation. The nematic-isotropic transition temperature T_{NI} for pure 8CB is 40.5°C [12]. The temperature T_C of the colder aluminum block is kept below T_{NI} by using a circulating water bath (Lauda model RCS-20D), while the temperature T_H of the hotter aluminum block is kept higher than T_{NI} with the use of a Tronac PTC-41 temperature controller. The laboratory temperature is kept at 20 ± 1 °C. Our oven is thermally insulated from the environment. Typically, rapid temperature fluctuations in the ovens are of the order of ±0.01 °C. These fluctuations are integrated out and have no effect on the thermal stability of the interface. However, slow temperature drifts can cause undesirable interface motions, making reliable comparison with theory impossible. Such drifts have to be kept as small as possible. Typical slow temperature drifts are of the order of 0.02 °C/h. Such temperature drifts impose an upper limit on the experimental observation time to about 1 to 2 h, depending on the sample. This in turn imposes a lower limit on the growth velocities that can be used, since the characteristic time for achieving the steady state is of the order of D/V^2, as mentioned in Sec. II. Impurities with smaller diffusion coefficients D are more suitable in this case. For the experiments of 8CB doped with hexachloroethane the smallest pulling velocity used was equal to 0.11 μm/s.

C. Temperature profile along the sample

A temperature gradient is established along the sample due to the difference in temperature between the two aluminum blocks. If one considers heat transport along the z direction of the sample only, with the sample at rest in the oven, the temperature gradient should be $G_0=(T_H-T_C)/l$, where $l=1.1$ cm is the separation between the blocks. Since there is also some heat transport normal to the sample, static gradients measured at the middle of the furnace are around 60% of G_0. Temperature profiles for different pulling velocities are shown in Fig. 3. These were generated by running a dummy cell with a thermocouple throughout the oven. The measured temperature gradients vary from 9.0 K/cm for $V_p=0$ to 8.0 K/cm for $V_p=51\mu$m/s; the temperature at the middle of the furnace varied by around 0.8 K when the pulling velocity was changed from $V_p=0$ to $V_p=51$ μm/s.

In previous experiments on directional solidification the variation of temperature at a given position in the furnace was not an important issue as the main interest was on the evolution of the instability after the interface had reached an essentially steady state. In this case, the value of the temperature gradient is important. In the present work, stationarity of the temperature field $T(z)$ is a crucial issue since we are interested in the displacement of the interface caused by the change in its melting temperature, due in turn to segregation of impurities in a fixed, imposed temperature profile. If the temperature profile changes as we pull the sample, we cannot attribute the recoil of the interface to impurity effects alone. This ''thermal effect'' imposes restrictions on the maximum pulling speed that we can use. A more sensitive way to measure this effect consists of waiting for the interface position to achieve the steady state for a given pulling velocity, and then changing this velocity. From the analysis developed in Sec. II, the steady-state interface position (Δz_S) should not

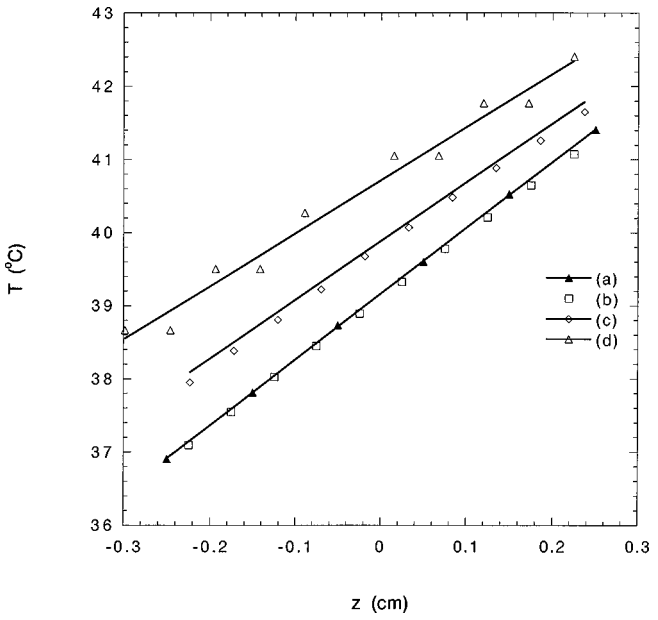

FIG. 3. Temperature profiles in the sample, for different pulling velocities. The center of the oven is at $z=0$, and $G=9.0$ K/cm. Profiles were generated by running a dummy cell with a thermocouple throughout the oven; (a) is for $V_p=0$; (b) is for $V_p=2.0$ μm/s; (c) is for $V_p=51.2$ μm/s; (d) is for $V_p=104.6$ μm/s. Profiles vary with pulling velocity. For $V_p \leqslant 2.0$ μm/s they are reasonably constant.

depend on the pulling velocity [see Eq. (15)]. Any change in the steady-state interface position is therefore due a change in the local temperature. Figure 4 shows the displacement of the steady-state interface position (Δz_S) as a function of pulling velocity, for a temperature gradient of 13.6 K/cm. The data points are well fit by a straight line with slope of 15.6 s, indicating that this is a characteristic time for heat conduction through the sample. If we assume that the main heat transport from the ovens throughout the sample is vertical, the value for the heat diffusion coefficient of the glass $D=5\times10^{-3}$ cm^2/s, and 15.6 s for the characteristic time, we obtain 4 mm for the total thickness of the sample. This is twice the actual value, indicating that the complete heat transport problem is more involved. The measurements of Fig. 4 are therefore important to determine the displacement of the interface due to this thermal effect. We choose the maximum working pulling velocity by requiring that the thermal effect cannot displace the interface more than 5% of the steady-state value for a particular sample. As an example, for a sample of 8CB doped with 1.1% molar of hexachloroethane and for a temperature gradient of 9 K/cm, the total displacement of the interface is around 80 μm. If we impose a maximum interface displacement due to this thermal effect of 4 μm, then the maximum pulling velocity should be around 0.3 μm/s. Therefore, from the considerations of the two last subsections, the optimal pulling velocity range in this case is 0.1 μ m/s$\leqslant V_p \leqslant$0.3 μm/s.

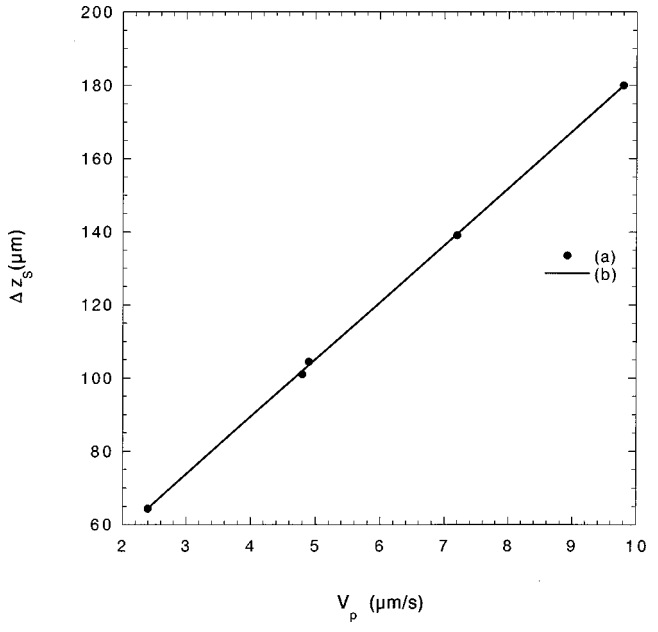

FIG. 4. Plot of steady-state interface position (Δz_s) as a function of pulling velocity (V_p) for $G=13.6$ K/cm; (a) is the experimental points and (b) is a data linear fit, where $\Delta Z_S=26.9+15.6\times V_p$. The steady-state interface position should be independent of pulling velocity [see Eq. (15)]. The change in Δz_s is due to the temperature profile change in the sample. This represents an undesirable ''thermal effect.''

IV. RESULTS AND DISCUSSION

A. 8CB doped with C_2Cl_6

In order to test the Warren-Langer model and our two-sided version of it for the recoil of a planar interface, we use a binary mixture of 8CB and 1.1% molar of C_2Cl_6. Such a binary mixture was chosen because the values for most of its parameters are available in the literature [8]. The experiment consists of pulling a sample with this binary mixture through a directional solidification oven. Initially the interface is at rest, and we set this position to $\Delta z=0$. At $t=0$ we start to pull the sample and follow the recoil of the interface as a function of time. Figure 5 shows a plot of the recoil of the interface as a function of time for three different pulling velocities. The symbols are the data and continuous lines are fittings using our two-sided version of the Warren-Langer model described in Sec. II. In the fitting procedure we fixed the value for the impurity concentration since it is known. The liquidus slope is related to the segregation coefficient through the van t'Hoff relation

$$m=\frac{RT_{NI}^2}{L}(1-k), \tag{16}$$

where $R=8.31$ J/mol K is the ideal gas constant, $T_{NI}=313.5$ K is the nematic-isotropic transition temperature for the pure system, $L=6.12\times10^2$ J/mol the latent heat of the nematic-isotropic transition, and k is the segregation coefficient. Also note that the diffusion coefficient of the impurity in the isotropic phase (D_I) is around twice its value in the nematic phase (D_N) [8]. Therefore, only k and D_I are varied during the fitting procedure. In Table I we show the parameters obtained from these fittings. If we used the one-sided version of Warren and Langer, we would obtain unrealistically large values for the impurity diffusion coefficient. The values displayed in Table I are consistent with the values obtained by other methods [8]. Therefore, our two-sided ver-

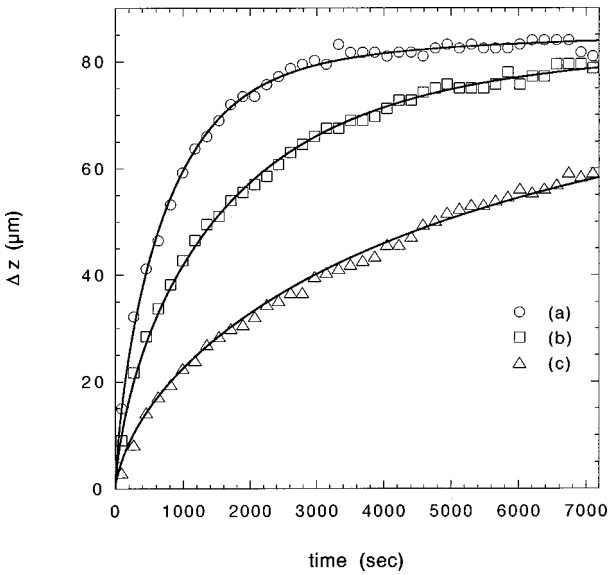

FIG. 5. Measured interface position as a function of time for $G=8.9$ K/cm and three different pulling velocities; (a) is for $V_p=0.32$ μm/s; (b) is for $V_p=0.23$ μm/s; (c) is for $V_p=0.11$ μm/s. Lines are fittings using our double-sided model. Fitting parameters are shown in Table I.

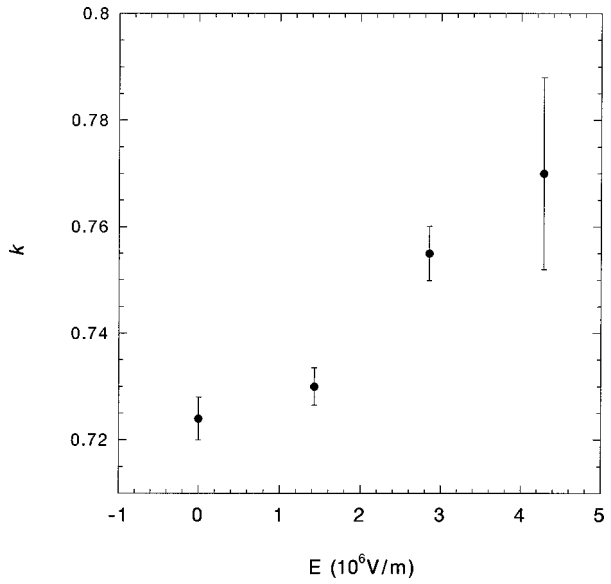

FIG. 6. Experimental values for the segregation coeficient k of the liquid crystal 8CB doped with water as a function of applied electric field E.

sion of the Warren-Langer analysis can describe very well the recoil of the nematic-isotropic interface of the $8CB/C_2Cl_6$ binary mixture, and gives good quantitative results for the segregation and diffusion coefficients of C_2Cl_6 in 8CB. This technique can be used for other binary systems.

B. Effect of applied electric field

One application of the technique presented above is the possibility of accurately measure the segregation coefficient of binary mixtures. One of the interesting features of the nematic-isotropic interface is that the degree of order in both phases can be changed by applying an electric field. We expect the segregation coefficient of impurities to be sensitive to such a change.

We made a sample by using glass slides covered with SnO_2 transparent electrodes [11]. This sample allows us to apply electric fields perpendicular to the sample, along the homeotropic direction. We then study the evolution of the planar nematic-isotropic interface and measure the segregation coefficient as a function of applied electric field, as described in the previous sections.

The sample thickness is 3.5 μm. In order to avoid electrolysis, we applied a sinusoidal voltage with frequency of 100 Hz, which seemed to give the best response, even though we have not made a systematic study of the frequency dependence of this effect. To avoid damaging of the sample, the maximum electric field used was 4.2×10^6 V/m. After applying this maximum electric field the temperature of the sample increases around 0.01 K. It causes a 10 μm displacement of the interface position that comes to rest around 6 min later. To make sure that we initiate a run with a still interface position we wait for 30 min after we apply the electric field. Figure 6 shows a plot of the measured segregation coefficient as a function of electric field, indicating that the segregation coefficient increases with increasing electric field. We could not use samples doped with hexacloroethane because they seemed to deteriorate very fast in presence of the tin oxide electrodes. Then we used one sample with water absorbed as impurity resulting in a segregation coefficient $k\approx0.74$, in agreement with measurements of Figueiredo *et al.* obtained from the cellular instability [9].

When we apply an electric field to a nematic liquid crystal, the order parameter increases in both the nematic and isotropic phases. Lelidis *et al.* [13,14] considered a Landau–de Gennes free energy for a homeotropic configuration of a nematic liquid crystal with a coupling between electric field and order parameter quadratic in the field (Kerr effect). They derived the phase diagram of the new phase transitions as a function of electric field. In particular, a new phase (the paranematic phase) appears, due to the ordering of the isotropic phase. From this free energy one can obtain an expression for the transition temperature, indicating that it increases with increasing electric field. Based on this free energy, we made a numerical calculation of the nematic (S_N) and isotropic (S_I) order parameters as a function of electric field, at the transition temperature (Fig. 7), which is the temperature of the interface for a pure system. Even though for a fixed temperature both S_N and S_I increase with electric field, at the transition temperature, which depends on the electric field as well, the difference between the nematic and isotropic order parameters decreases for increasing electric field.

TABLE I. Fitting parameters of the double-sided model for the interface position. The value marked with an asterisk was fixed in the fitting for the lowest velocity, since in this case the steady-state position value was not yet well defined. Note that $D_N=\frac{1}{2}D_I$.

V_p (μm/s)	D_I (μm^2/s)	k
0.11	39.0	0.93*
0.23	43.5	0.93
0.32	35.7	0.93
literature [8]	40.0	0.86–0.93

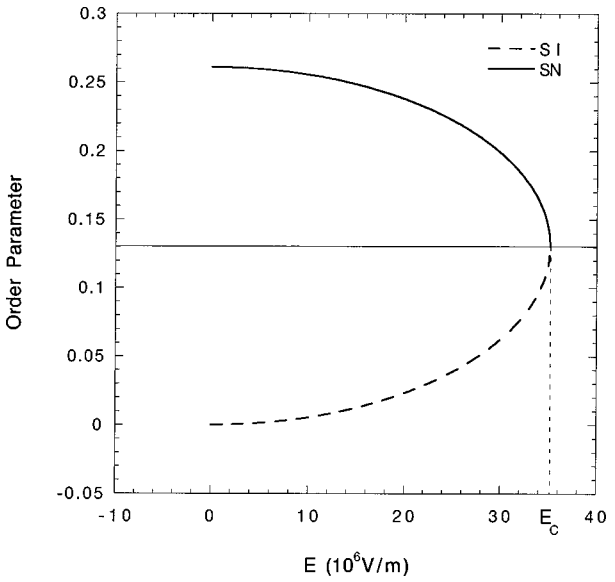

FIG. 7. Nematic (S_N) and isotropic (S_I) order parameters at the transition temperature as a function of electric field E in the Landau–de Gennes model with E^2 coupling to the order parameter. Full line is for S_N and dashed line is for S_I. E_C is the critical electric field where $S_N = S_I$.

At a critical electric field (E_c) the two phases will have identical order parameter values. Since in this situation there is no physical distinction between these phases, we then expect that the segregation coefficient of impurities becomes 1. Qualitatively, the segregation coefficient should be an increasing function of electric field, as observed experimentally. An attempt to explain these observations on a more quantitative basis is in progress.

We also made some preliminary experiments on the cellular instability of our liquid crystal samples under an electric field. An interesting preliminary result is that the capillary length of the pattern increases with applied electric field. We have the ability of continuously varying important parameters of the Mullins-Sekerka problem, such as the segregation coefficient, capillary length, and eventually surface tension anisotropy. This may help to clarify the physical origin of the unusually large capillary length observed in cellular instabilities of liquid crystals [9].

V. CONCLUSIONS

We have made careful measurements of the evolution of the recoil of the planar nematic-isotropic interface of the liquid crystal 8CB doped with C_2Cl_6. We extended the one-sided-Warren-Langer model for the recoil of planar interfaces, to the two-sided model of solidification and showed that this model fits our data very well and gives values for the segregation and diffusion coefficients of C_2Cl_6 in 8CB comparable to the ones found in the literature and measured by other methods. In addition, we measured the segregation coefficient as a function of applied electric field of 8CB doped with water and observed that it increases with increasing electric field. A qualitative explanation for this effect is given in terms of the Kerr effect in nematic liquid crystals. Preliminary experiments indicate that the capillary length of cellular instabilities in this system also increases with electric field. As far as we know, this is the first available binary system where the segregation coefficient and capillary length can be continuously varied. This opens up new possibilities in the study of pattern formation during cellular and dendritic instabilities.

ACKNOWLEDGMENTS

We acknowledge support from the Brazilian Agencies: Fundação de Amparo à Pesquisa do Estado de Minas Gerais (FAPEMIG) and Conselho Nacional de Desenvolvimento Científico e Tecnológico (CNPq). We are grateful to Dr. Alaíde P. Mammana from CTI–Campinas for providing us with glass slides covered with tin oxide.

[1] W. W. Mullins and R. F. Sekerka, J. Appl. Phys. **34**, 232 (1963); **35**, 444 (1964).
[2] James A. Warren and J. S. Langer, Phys. Rev. E **47**, 2702 (1993).
[3] J. D. Hunt, K. A. Jackson, and H. Brown, Rev. Sci. Instrum. **37**, 805 (1966).
[4] B. Caroli, C. Caroli, and L. Ramirez-Piscina, J. Cryst. Growth **132**, 377 (1993).
[5] R. Trivedi and K. Somboonsuk, Acta Metall. **33**, 1061 (1985).
[6] W. Losert, B. Shi, and H. Z. Cummins, Proc. Natl. Acad. Sci. USA **95**, 431 (1998); **95**, 439 (1998).
[7] P. Oswald, J. Bechhoefer, and A. Libchaber, Phys. Rev. Lett. **58**, 2318 (1987).
[8] J. Bechhoefer, A. J. Simon, and A. Libchaber, Phys. Rev. A **40**, 2042 (1989).
[9] J. M. A. Figueiredo M. B. L. Santos, L. O. Ladeira, and O. N. Mesquita, Phys. Rev. Lett. **71**, 4397 (1993).
[10] J. M. A. Figueiredo and O. N. Mesquita, Phys. Rev. E **53**, 2423 (1996).
[11] Fundadação Centro Tecnológico para Informática (CTI), Rodovia Dom Pedro I (SP 65), km143,6 - Campinas, SP, Brazil.
[12] Merck (old BDH) product information catalog, 1986 (unpublished).
[13] I. Lelidis, M. Nobili, and G. Durand, Phys. Rev. E **48**, 3818 (1993).
[14] I. Lelidis and G. Durand, Phys. Rev. E **48**, 3822 (1993).